Eur. Phys. J. C 11, 79–88 (1999)
Digital Object Identifier (DOI) 10.1007/s100529900157

THE EUROPEAN PHYSICAL JOURNAL C

Strangeness enhancement at midrapidity in Pb–Pb collisions at 158 A GeV/c: A comparison with VENUS and RQMD models

The WA97 Collaboration

F. Antinori[9], H. Bakke[2], W. Beusch[5], I.J. Bloodworth[4], R. Caliandro[1], N. Carrer[9], D. Di Bari[1], S. Di Liberto[11], D. Elia[1], D. Evans[4], K. Fanebust[2], R.A. Fini[1], J. Ftáčnik[6], B. Ghidini[1], G. Grella[12], H. Helstrup[3], A.K. Holme[8], D. Huss[7], A. Jacholkowski[1], G.T. Jones[4], J.B. Kinson[4], K. Knudson[5], I. Králik[6], V. Lenti[1], R. Lietava[6], R.A. Loconsole[1], G. Løvhøiden[8], V. Manzari[1], M.A. Mazzoni[11], F. Meddi[11] A. Michalon[13], M.E. Michalon-Mentzer[13], M. Morando[9], F. Navach[1], P.I. Norman[4], B. Pastirčák[6], E. Quercigh[5], G. Romano[12], K. Šafařík[5], L. Šándor[5,6], G. Segato[9], P. Staroba[10], M. Thompson[4], T.F. Thorsteinsen[2], G.D. Torrieri[4], T.S. Tveter[8], J. Urbán[6], O. Villalobos Baillie[4], T. Virgili[12], M.F. Votruba[4], P. Závada[10]

[1] Dipartimento I.A. di Fisica dell'Università e del Politecnico di Bari and Sezione INFN, Bari, Italy
[2] Fysisk institutt, Universitetet i Bergen, Bergen, Norway
[3] Høgskolen i Bergen, Bergen, Norway
[4] School of Physics and Astronomy, University of Birmingham, Birmingham, UK
[5] CERN, European Laboratory for Particle Physics, Geneva, Switzerland
[6] Institute of Experimental Physics, Slovak Academy of Sciences, Košice, Slovakia
[7] GRPHE, Université de Haute Alsace, Mulhouse, France
[8] Fysisk institutt, Universitetet i Oslo, Oslo, Norway
[9] Dipartimento di Fisica dell'Università and Sezione INFN, Padua, Italy
[10] Institute of Physics, Academy of Sciences of Czech Republic, Prague, Czech Republic
[11] Dipartimento di Fisica dell'Università "La Sapienza" and Sezione INFN, Rome, Italy
[12] Dipartimento di Scienze Fisiche "E.R. Caianiello" dell'Università and INFN, Salerno, Italy
[13] Institut de Recherches Subatomiques, IN2P3/ULP, Strasbourg, France

Received: 29 April 1999 / Published online: 14 October 1999

Abstract. Recently the WA97 Collaboration has measured K^0_S, Λ, Ξ, Ω and negative particle yields and transverse mass spectra at central rapidity in Pb–Pb and p–Pb collisions at 158 A GeV/c. These results are compared with the predictions of two of the most widely used event generators for heavy-ion collisions: VENUS 4.12 and RQMD 2.3. Both models predict that enhancements increase with the strangeness content of the particle. They fail, however, to reproduce completely the measured values of yields at central rapidity. In particular, for multistrange particles, VENUS fails to reproduce both the p–Pb and the Pb–Pb data, while RQMD works for p–Pb collisions but seems to be unable to reproduce the Ω data in Pb–Pb collisions. Moreover, the predicted behavior for strangeness production as a function of the centrality of the collision appears to be different from the observed behavior.

1 Introduction

The measurement of strange-particle yields provides one of the most promising ways to study the properties of nuclear matter at very high-energy densities. In particular, it has been suggested that the production of multistrange baryons would be enhanced if a quark gluon plasma (QGP) were formed [1]. In this scenario, strange-quark pairs would be easily produced, mostly from gluon–gluon interactions; as a consequence, strangeness production would be enhanced and it could rapidly reach its equilibration value. In a hadronic scenario, strangeness production is also expected to be enhanced in nucleus–nucleus interactions with respect to proton–proton and proton–nucleus interactions. The process, however, is expected to be slower; in particular, for multistrange particles, the equilibration time is expected to be longer than the system lifetime [1–3]. Therefore this mechanism should disfavor multistrange particles.

As a result of recent findings on strangeness production in heavy-ion experiments [4], it has become clear that nucleus–nucleus interactions cannot be described by a simple superposition of nucleon collisions, and that the nuclear medium has a strong influence on the observable quantities. A number of Monte Carlo models, based on conventional interactions and including the full dynamics of ultrarelativistic nuclear collisions, have been proposed. Such models are able to produce quantitative predictions;

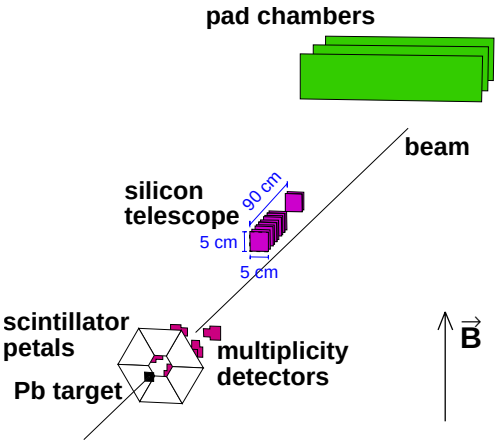

Fig. 1. The WA97 setup

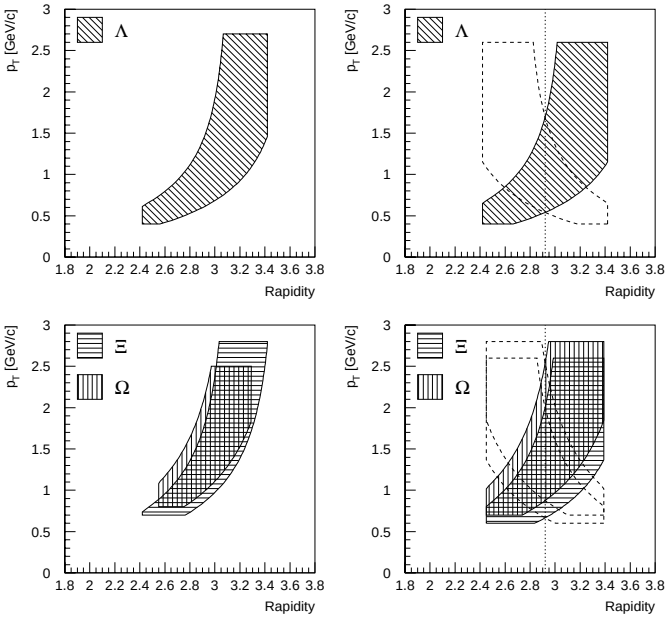

Fig. 2. Acceptance windows for Λ, Ξ, and Ω hyperons for p–Pb (left) and Pb–Pb (right) interactions. For Pb–Pb collisions, the symmetry of the system around midrapidity ($y_{\rm cm} = 2.91$) allows one to symmetrize the acceptance windows by reflection around $y_{\rm cm}$. The reflected windows are drawn with dashed lines

therefore, they deserve careful comparison to the experimental data.

Recently, measurement of multistrange- baryon production has been carried out by the WA97 Collaboration for Pb–Pb and p–Pb interactions at 158 A GeV/c [5]. In this paper, we shall compare these data with the predictions of two Monte Carlo models: VENUS [6] and RQMD [7], which are amongst the most frequently used event generators and for most successful microscopic models available [8].

Some of the results concerning VENUS have been already presented in [9].

2 The WA97 experiment

The WA97 setup, shown schematically in Fig. 1, is described in detail in [10]. The target and the silicon telescope were placed inside the homogeneous 1.8 T magnetic field of the CERN Omega magnet.

The 158 A GeV/c lead beam from the CERN SPS was incident on a lead target with a thickness corresponding to 1% of an interaction length. Scintillator petal detectors behind the target provided an interaction trigger selecting approximately the most central 40% of the Pb–Pb collisions. Two planes of microstrip multiplicity detectors covering, for all $p_{\rm T}$ values, the pseudorapidity region $2 \lesssim \eta \lesssim 3$ and $3 \lesssim \eta \lesssim 4$ respectively, provided information for more detailed off-line study of the centrality dependence of particle ratios and spectra.

In the proton reference runs at 158 GeV/c, data were collected with two different trigger conditions:

(a) at least two tracks in the telescope, necessary for finding neutral strange particles (V^0); and
(b) at least one track in the telescope.

Sample (a) was used for the strange-particle study and sample (b) for the study of negative hadrons (h^-). In both cases, the effect of the trigger was taken into account in the calculation of the particle yields.

The Λ, Ξ^-, and Ω^- hyperons and their antiparticles were identified by the reconstruction of their decays into final states containing only charged particles:

$$\begin{aligned}
\Lambda &\to {\rm p} + \pi^- \\
\Xi^- &\to \Lambda + \pi^- \\
&\quad\hookrightarrow {\rm p} + \pi^- \\
\Omega^- &\to \Lambda + {\rm K}^- \\
&\quad\hookrightarrow {\rm p} + \pi^-
\end{aligned}$$

The $\rm K^0_S$ were identified by the decay

$$\rm K^0_S \to \pi^- + \pi^+$$

We selected as h^- negative tracks which pointed to the interaction vertex.

The details of the analysis, i.e., the extraction of the various particle signals and the weighting procedures are discussed in [5,11,12].

The acceptance windows for Λ, Ξ and Ω from p–Pb and Pb–Pb collisions are shown in Fig. 2. In Fig. 3 are shown those for h^- and $\rm K^0_S$.

The multiplicity detectors allow us to study particle yields as a function of collision centrality as measured by the number of participants. To this purpose the multiplicity spectrum is divided into four bins, and the average number of participants for each bin is calculated as described in [5]. For p–Pb, the number of participants corresponds to the estimated average for minimum bias collisions. The particle production yield per event, Y, in each centrality bin is defined by the integral

$$Y = \int_0^\infty {\rm d}p_{\rm T} \int_{y_{\rm cm}-0.5}^{y_{\rm cm}+0.5} {\rm d}y \, \frac{{\rm d}^2 N}{{\rm d}y \, {\rm d}p_{\rm T}} \qquad (1)$$

where y is the rapidity ($y_{\rm cm}$ being the midrapidity value) and $p_{\rm T}$ is the transverse momentum. The extrapolation to

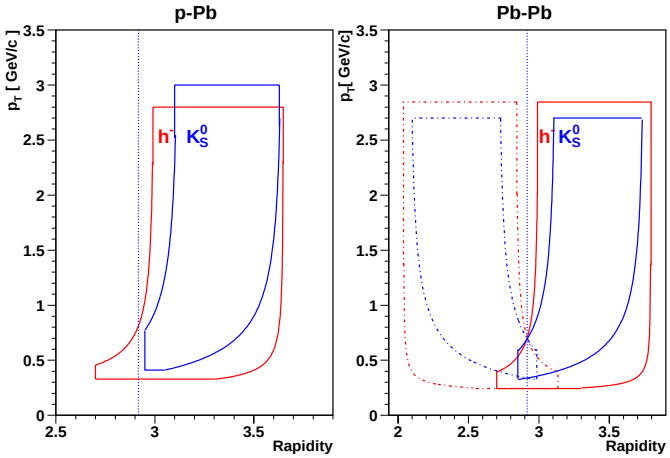

Fig. 3. Acceptance windows for h^- (assumed to be pions) and K^0_S

the window $|y-y_{cm}| < 0.5$ and $p_T > 0$ GeV/c is performed according to expression (2) using the values of T given in [12]:

$$\frac{d^2N}{dm_T\,dy} = f(y)\,m_T^{3/2}\,\exp\left(-\frac{m_T}{T}\right) \qquad (2)$$

where $m_T = \sqrt{m^2+p_T^2}$ is the transverse mass. For the present analysis, with limited statistics the rapidity distribution is assumed to be flat for $|y-y_{cm}| < 0.5$. The fit was performed with the method of maximum likelihood.

3 The models

A complete description of the very energetic nuclear scattering (VENUS) model can be found in [6]; here we shall present a summary of its main ideas.

The model is based on the phenomenological Gribov–Regge Theory (GRT) of hadron–hadron and nucleus–nucleus interactions. According to GRT, the basic interaction mechanism is Pomeron exchange, in which a Pomeron need not describe a real particle, but has some well-defined properties. The Pomeron exchange could be connected to the color exchange mechanism, on which several models are based (such as the dual parton model [13]).

The model contains some parameters which are tuned in order to reproduce the experimental quantities. For example, string decay is governed by a set of parameters tuned to reproduce hadron production in e^+e^- and lepton–nucleus collisions, whereas string interaction parameters come from hadron–hadron data. When nuclear interactions are involved, additional parameters are introduced to describe the nuclear density and the rescattering process for particles in nuclear matter. All the parameters are fixed from the available data on leptonic and hadronic interactions [6].

The relativistic quantum molecular dynamics (RQMD) model [7] is based on the Lund model of hadronic interactions [14]. The interaction mechanism is based on the string momentum exchange, which is at first approximation equivalent to the color exchange. However, in the momentum exchange model, the strings are formed by the same quarks as those of the original nucleons, whereas in the color exchange process, strings can be formed with quarks coming from different nucleons.

The string decay is provided by a procedure that is slightly different with respect to VENUS. The main difference is that one of the two decay substrings always has to be a stable particle, for which no further fragmentation is allowed.

In RQMD, strings which overlap in nuclear matter at high density do not fragment independently of each other, but they can interact, leading to color rope formation. Ropes can be viewed as a model of locally deconfined quark matter.

In the rescattering stage of nuclear reactions, the interaction probabilities in RQMD are set from the measured hadronic cross sections or estimated via several hadronic interaction models. Therefore no additional free parameters are introduced at this stage.

Both models are able to reproduce the main features of events, such as multiplicity, rapidity, and transverse momentum distributions for pions and nucleons in hadron–hadron, hadron–nucleus, and nucleus–nucleus interactions, at both Brookhaven (AGS) and CERN (SPS) energies. They are also able to reproduce multiplicity and rapidity distributions of some strange particles like Λ and K in several interactions [6,15].

It is important to stress that both models predict some strangeness enhancement in nucleus–nucleus interactions with respect to nucleon–nucleon or nucleon–nucleus collisions. In VENUS, the increase of strangeness is related to the multiple Pomeron exchange, which is more probable at high nuclear density. In RQMD, the enhancement comes from multiple collisions of formed hadrons, which modify their quark content. An important additional contribution comes, however, from the existence of color rope decay, since strange-quark production can be easily enhanced by increasing the rope field strength.

Table 1. Statistics of events generated by VENUS and RQMD

	p–Pb	Pb–Pb	Pb–Pb with trigger
VENUS 4.12	500 000	20 000	8029
RQMD 2.3	500 313	20 611	8166

4 Comparison with experimental results

In order to compare the predictions of these models with WA97 data, we generated p–Pb and Pb–Pb events at 158 A GeV/c using the standard VENUS 4.12 and RQMD 2.3 versions, without modification of internal parameters. We let all resonances decay and kept in the final state all the strange particles that are stable under strong and electromagnetic interactions. The statistics of the generated samples are reported in the first two columns of Table 1; the experimental data samples from WA97 consist

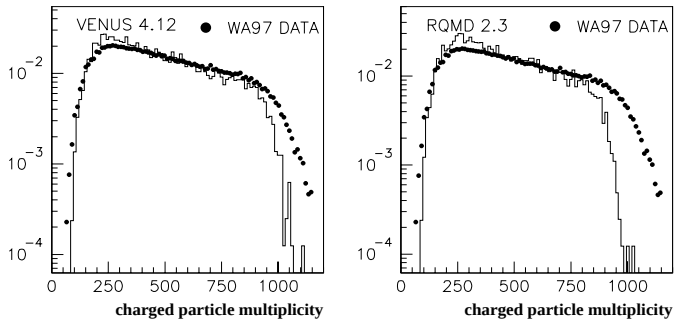

Fig. 4. Charged multiplicity distributions produced by VENUS and RQMD with the experimental trigger condition included. The corresponding distribution measured by the WA97 experiment is represented by black dots

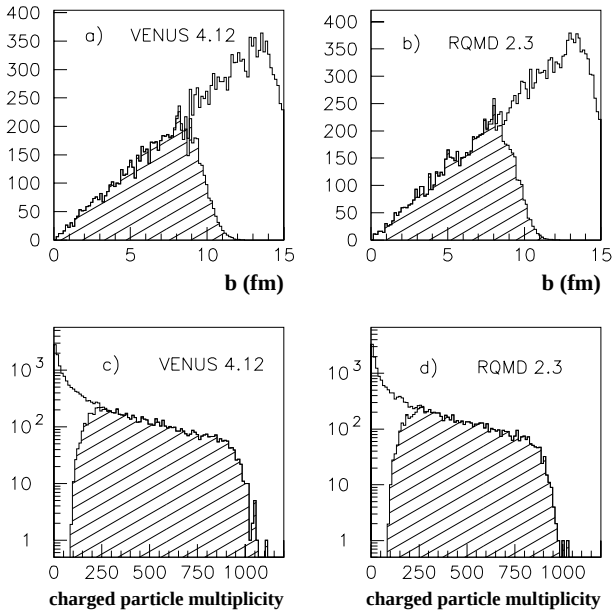

Fig. 5a–d. Impact parameter distributions (**a**,**b**) and charged-particle multiplicity distributions (**c**,**d**) for Pb–Pb events generated by VENUS and RQMD. The shaded regions denote the events selected by the centrality trigger

of about 120 million p–Pb events and about 200 million Pb–Pb events at the same energy.

To reproduce the centrality trigger required for Pb–Pb data, we followed the particles produced in the simulation through the experimental setup by GEANT [16].

In Fig. 4, the charged multiplicity distributions obtained by the models are compared with experiment. Apart from the high multiplicity regions, both models reproduce the data reasonably. It is worth noting that the effect of the trigger has been adequately modeled.

In Fig. 5, the impact parameter of the collisions (a, b) and the charged particle multiplicity distributions (c, d) are shown for Pb–Pb events generated by VENUS and RQMD. The shaded regions denote the events that satisfy the Pb–Pb centrality trigger ($\sim 40\%$). The number of such events is reported in the third column of Table 1; they represent the statistics used in the comparison with Pb–Pb data.

Table 2. Number of particles generated by VENUS and RQMD in p–Pb and Pb–Pb interactions (with centrality trigger) inside their respective kinematic regions

	p–Pb		Pb–Pb	
	VENUS	RQMD	VENUS	RQMD
h^-	268287	209070	542737	565627
K^0_S	12038	10713	36652	45215
Λ	10673	9078	23552	33291
$\overline{\Lambda}$	3559	2592	9104	4814
Ξ^-	882	305	3763	2726
$\overline{\Xi}^+$	447	119	2092	811
Ω^-	176	10	971	128
$\overline{\Omega}^+$	123	9	815	78

The physical quantities used for the comparison are: (a) the inverse slopes of the transverse mass distributions; and (b) the particle production yields Y, as defined in Sect. 2 both for the strange particles K^0_S, Λ, $\overline{\Lambda}$, Ξ^-, $\overline{\Xi}^+$, Ω^-, $\overline{\Omega}^+$ and for negative charged particles coming from the target (h^-), which we treat as pions.

The inverse slopes were determined in the WA97 kinematic windows by application of the same fit procedure to the Monte Carlo data, as was done for the experimental data. Details on this procedure are reported in [5] and [11]. The transverse mass distributions were parametrized according to expression (2), where T is the inverse slope parameter, to be fitted.

The particle yields for the generated events were evaluated in the kinematic windows as used for the data; the result was then extrapolated to the common window $|y - y_{\rm cm}| < 0.5$ and $p_{\rm T} > 0$ GeV/c using expression (1). The number of generated particles, counted inside their respective kinematic windows for p–Pb and Pb–Pb interactions simulated by VENUS and RQMD, is shown in Table 2.

In addition, for each particle species we compute a global enhancement, going from p–Pb to Pb–Pb collisions, defined as

$$\frac{\langle Y\rangle_{\rm Pb--Pb}}{\langle Y\rangle_{\rm p--Pb}} \qquad (3)$$

where $\langle Y\rangle$ are the average yields over the full centrality range covered by the experiment, calculated in the common window. The enhancement at midrapidity for the various hadron species predicted by the models were then compared to the measured ones.

4.1 p–Pb interactions

In Fig. 6 the measured yields in p–Pb are compared with the predictions of VENUS and RQMD. Both models appear to reproduce well the yields for negatives, K^0_S and Λ. For Ξ and Ω, however, an overestimation by VENUS with respect to data is observed, which is larger for Ω than

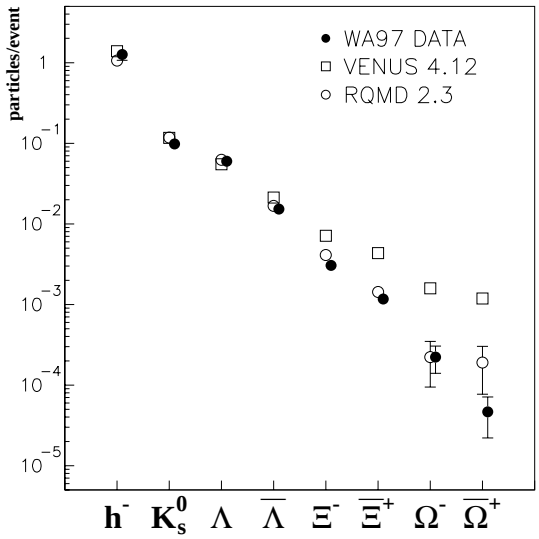

Fig. 6. Particles per p–Pb interaction measured by the WA97 experiment (black dots), compared with the yields predicted by VENUS (open squares) and RQMD (open circles)

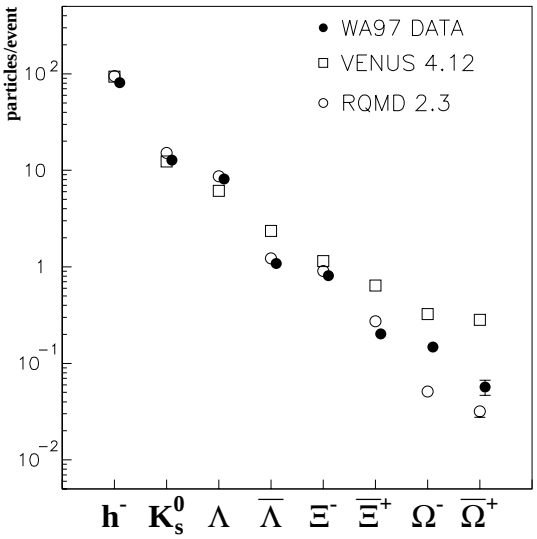

Fig. 8. Particles per Pb–Pb triggered event measured by the WA97 experiment (black dots), compared with the yields predicted by VENUS (open squares) and RQMD (open circles)

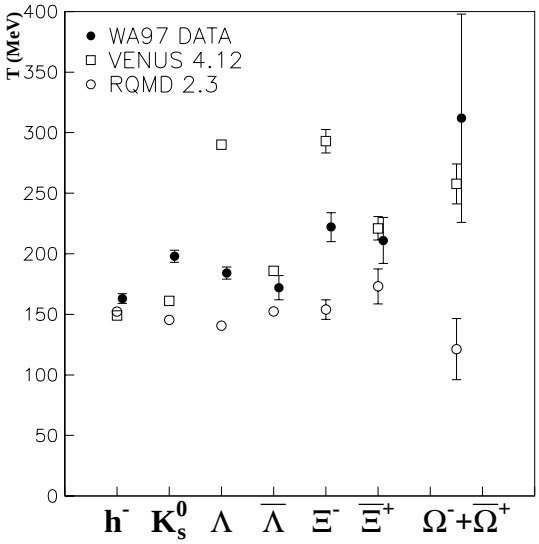

Fig. 7. Inverse slopes measured by the WA97 experiment in p–Pb interactions (black dots), compared with the ones predicted by VENUS (open squares) and RQMD (open circles)

for Ξ and for antiparticles than for particles. The differences are as large as one order of magnitude for Ω^- and $\overline{\Omega}^+$, as was already pointed out in [9]. The predictions of the RQMD model, on the other hand, are in satisfactory agreement with data for all the particles considered.

In Fig. 7, the inverse slopes for the different particles are displayed, for both models and for the WA97 data. Ω^- and $\overline{\Omega}^+$ were put together because of the low statistics of the experimental sample. With the exception of h^-, $\overline{\Lambda}$ and $\overline{\Xi}^+$, substantial discrepancies are observed for the inverse slopes. For VENUS, these discrepancies were already observed in p–Ar and p–Xe interactions for K^0_S and Λ [6] and in p–Pb interactions for Λ and Ξ^- [9]. It can be noted that RQMD predicts the same inverse slope value of about 150 MeV for all the particles considered, with perhaps a slightly lower value for $\Omega^- + \overline{\Omega}^+$. VENUS predicts a slight increase of inverse slopes with the particle mass, with the exception of Λ and Ξ^-, which stray significantly from this trend toward higher values.

4.2 Pb–Pb interactions

The comparison of the particle yields obtained in the triggered Pb–Pb events is shown in Fig. 8. The agreement with data is satisfactory for negatives and K^0_S and Λ yields for both models. VENUS overestimates the yields of $\overline{\Lambda}$ and multistrange particles, reaching a disagreement of one order of magnitude for $\overline{\Omega}^+$. On the other hand, RQMD is in satisfactory agreement for $\overline{\Lambda}$, Ξ^-, and $\overline{\Xi}^+$, while it underestimates Ω^- and $\overline{\Omega}^+$ production by about a factor of 2.

The comparison of inverse slopes, shown in Fig. 9, reveals a general agreement of both models with WA97 data, in the sense that they show the same rise from h^- through K^0_S to Λ and then a flattening. For the multistrange baryons, VENUS tends to overestimate while RQMD underestimates. In general, RQMD predictions reproduce fairly well all the measured inverse slopes, as has already been pointed out in [17].

4.3 Strangeness enhancement

In Fig. 10 the enhancements for WA97 data, VENUS, and RQMD are shown. They were determined from (3) in the common window $|y - y_{\rm cm}| < 0.5$ and $p_{\rm T} > 0$ GeV/c.

One notices that both models predict that enhancements increase with the strangeness content of the particle, a trend which is also observed in the data. RQMD

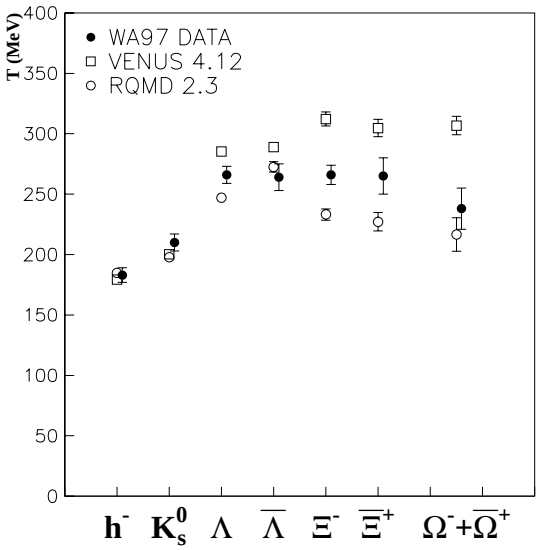

Fig. 9. Inverse slopes measured by the WA97 experiment in Pb–Pb interactions (black dots), compared with the ones predicted by VENUS (open squares) and RQMD (open circles)

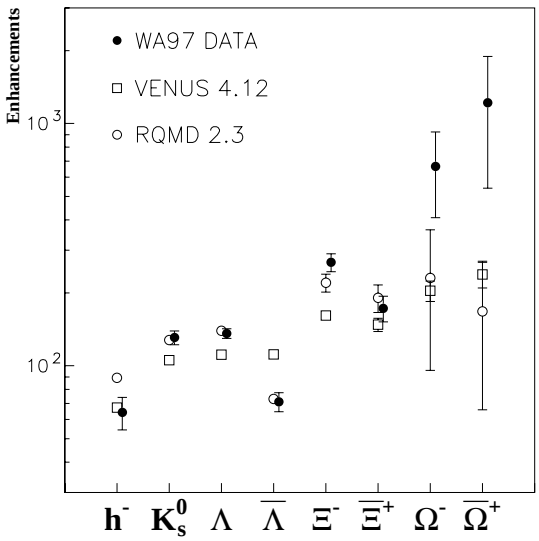

Fig. 10. Strangeness enhancements in Pb–Pb collisions with respect to p–Pb interactions for WA97 data (black dots), VENUS (open squares) and RQMD (open circles)

is able to reproduce the measured enhancements of K^0_S, Λ, $\overline{\Lambda}$, Ξ^-, and $\overline{\Xi}^+$, though at the price of overestimating the enhancement of negatives. The Ω^- and $\overline{\Omega}^+$ enhancements are, however, still underestimated, the discrepancy being within two standard deviations. For VENUS, the agreement is better for the negatives but worse for strange particles.

Figure 11 shows the enhancements relative to negative particles (h^-) for strange baryons (Fig. 11a) and antibaryons (Fig. 11b). It is interesting to observe that in the data, the enhancements are larger for Λ and Ξ^- than for $\overline{\Lambda}$ and $\overline{\Xi}^+$. Such a trend is present in RQMD, but not in

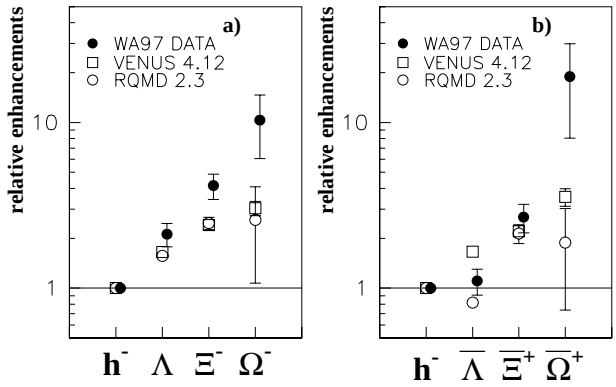

Fig. 11a,b. Relative enhancements for **a** strange baryons, and **b** strange antibaryons, relative to the enhancement of negatives

VENUS, which predicts a similar increase for baryons and antibaryons.

4.4 Centrality dependence of the enhancements

The WA97 Collaboration has studied particle production at central rapidity in Pb–Pb collisions as a function of the centrality of the collision. To this purpose, the mean number $N^{\rm G}_{\rm part}$ of nucleons participating in the collision has been used as a measure of the centrality. $N^{\rm G}_{\rm part}$ was estimated from the multiplicity measurements using a Glauber model, as mentioned in Sect. 2.

In order to compare the centrality dependence predicted by VENUS and RQMD with the one observed by our experiment, we fitted the multiplicity distributions given by the two models, shown in Fig. 4, with the Glauber model. The number of participants $N^{\rm G}_{\rm part}$ in VENUS and RQMD-generated Pb–Pb collisions were then calculated with the same procedure used for real data.

The results are summarized in Fig. 12. Figures 12a,c,e show the particle yields expressed in units of the corresponding yield per p–Pb interaction for the WA97 data, VENUS, and RQMD, respectively. The particle yields in Pb–Pb correspond to four ranges of charged multiplicity covered by the experiment (Fig. 4) and are compared to a yield curve (full line) drawn through the p–Pb point and proportional to $N^{\rm G}_{\rm part}$. The value of $N^{\rm G}_{\rm part}$ for p–Pb interactions used for real data corresponds to minimum bias collisions and was kept equal in VENUS and RQMD simulated events.

Here again we observe that both models and data show an increase of yields from p–Pb to Pb–Pb collisions and from strange to multistrange particles. It appears inadequate to describe the data from p–Pb to Pb–Pb with a simple power law. Therefore we restrict ourselves to the Pb–Pb data. Thus a fit has been performed in order to compare quantitatively data and models which assumes a power law dependence $(N^G_{\rm part})^\beta$. We shall see that this assumption is not strictly valid for VENUS, and should be taken with caution when applied to data. The dashed lines are the results of the fit made through the Pb–Pb data

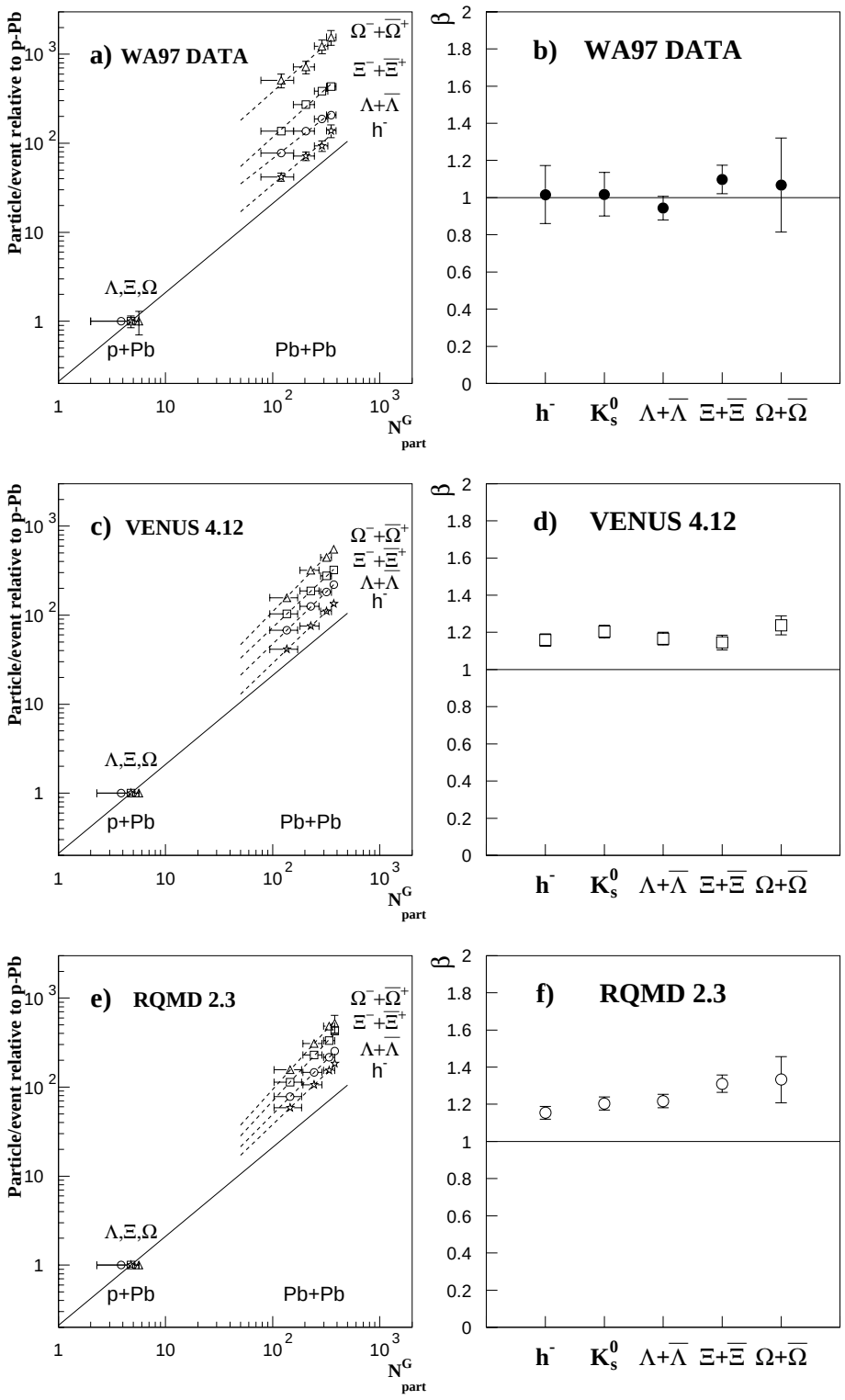

Fig. 12a–f. The h^-, Λ, Ξ, and Ω yields expressed in units of yields observed in p–Pb collisions as a function of the number of participants $N^{\rm G}_{\rm part}$ for WA97 data **a**, VENUS **c**, and RQMD **e**. The full line represents a function proportional to the number of participants and the dashed lines are the results of a power law fit $(N^G_{\rm part})^\beta$ made through the Pb–Pb points. In **b**,**d**,**f** are reported the fitted values of the exponent β, for WA97 data, VENUS, and RQMD, respectively

points only. Figures 12b,d,f show the fitted values of β for all particle species for WA97 data, VENUS, and RQMD, respectively. The experimental values of β (Fig. 12b) are all consistent with unity ($\chi^2/{\rm ndf} = 0.63$), suggesting that in the centrality range covered by the WA97 experiment, all the Pb–Pb yields increase linearly with $N^{\rm G}_{\rm part}$ [5]. Moreover, the fact that all Pb–Pb points in Fig. 12a lie above the full line ($\beta = 1$) suggests that between the p–Pb and Pb–Pb points, there is a centrality range within which yields grow more quickly than linearly with $N^{\rm G}_{\rm part}$. This hints that all the reported enhancements saturate for some value of $N^{\rm G}_{\rm part}$ below the lower limit of the covered centrality interval.

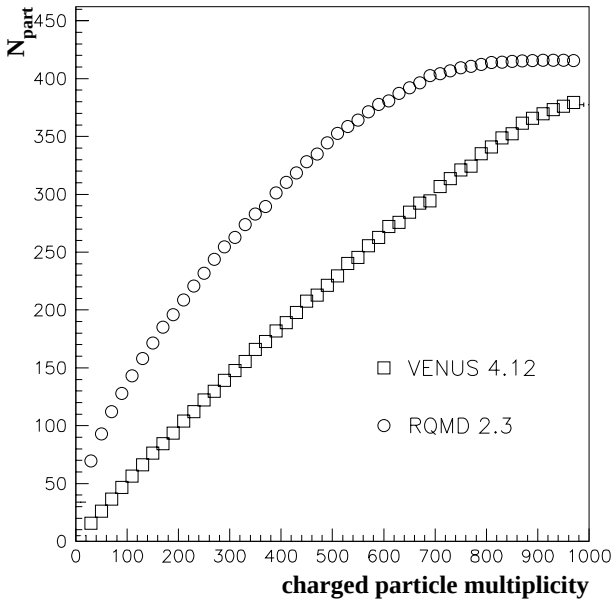

Fig. 13. Correlation of the number of participants with the charged-particle multiplicity in the interval $2 < \eta < 4$ for VENUS (open squares) and RQMD (open circles)

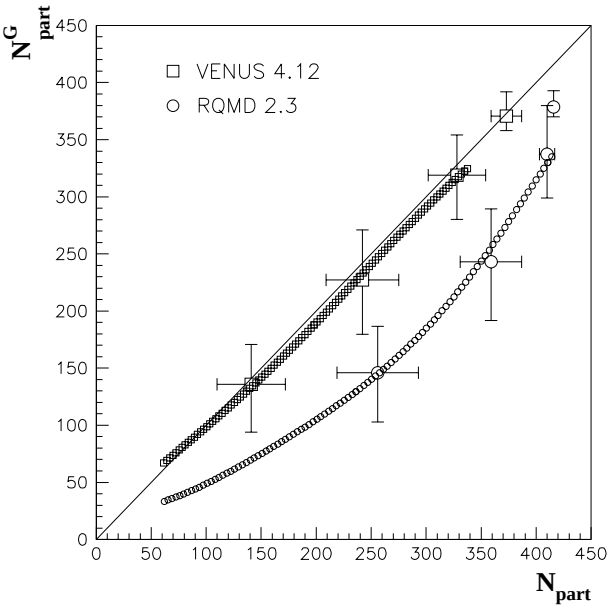

Fig. 14. Correlation between the number of participants in VENUS (open squares) and RQMD (open circles) estimated by use of the Glauber model calculation ($N_{\rm part}^{\rm G}$) and those directly supplied by the models themselves ($N_{\rm part}$). The full line indicates the diagonal, and the points refer to the mean values of the number of participants calculated in the four centrality bins used by WA97

On the other hand, in Figs. 12d,f, for VENUS and RQMD, the fitted values of β for all particle species are significantly larger than unity, indicating that the Pb–Pb Monte Carlo yields continue to increase with centrality faster than $N_{\rm part}^{\rm G}$ within the centrality range of the WA97 experiment. For RQMD, the fitted lines seem to point to the p–Pb common value, thus suggesting a continuous increase of the particle yields with centrality; this is in clear disagreement with the scenario depicted by data. For VENUS, instead, a change in slope appears to still be necessary to describe the full range of centrality from p–Pb to Pb–Pb.

5 Centrality dependence in the models

For a better understanding of the centrality dependence of strangeness production predicted by the models, we removed the trigger condition applied to the simulated events, so that we can investigate the full centrality range of Pb–Pb collisions (hereafter, these events will be referred to as "minimum bias events"). For this study, the centrality of the collision is estimated by the use of the value of the number of participants directly supplied by the models ($N_{\rm part}$) and not by a Glauber analysis as done previously. This allows us to investigate the dependence of the predictions on the various centrality scales proposed.

The correlations between the number of participants and the charged- particle multiplicity in the interval $2 < \eta < 4$ for VENUS and RQMD are shown in Fig. 13. From this figure it can be seen that for multiplicities lower than about 800, VENUS shows a linear dependence between $N_{\rm part}$ and the charged-particle multiplicity, as is assumed by the Glauber model, while RQMD deviates from this trend and produces fewer charged particles per participant.

Another way of seeing this is to look at the correlation between the number of participants of the models, estimated by use of the Glauber model calculation ($N_{\rm part}^{\rm G}$), and the number of participants directly supplied by the models ($N_{\rm part}$). The two correlations, for VENUS and RQMD, are shown in Fig. 14. The RQMD correlation substantially deviates from the diagonal, indicating that the centrality scales of VENUS and RQMD as defined by $N_{\rm part}$ are different: We will call them $N_{\rm part}^{\rm VENUS}$ and $N_{\rm part}^{\rm RQMD}$, respectively. It is worth noting that this difference arises from the different definition of "participant" in the two models: While $N_{\rm part}^{\rm VENUS}$ counts only nucleons which undergo primary collisions, $N_{\rm part}^{\rm RQMD}$ include also nucleons involved in secondary interactions.

The particle yields generated by VENUS and RQMD for Pb–Pb minimum bias collisions are shown respectively in Fig. 15 as a function of $N_{\rm part}^{\rm VENUS}$ and in Fig. 16 as a function of $N_{\rm part}^{\rm RQMD}$. The last four yield points fall in the centrality range covered by the WA97 experiment; the full symbols indicate the corresponding yields in p–Pb collisions. From the two figures, it can be concluded that both models predict a continuous increase of negatives and strange particles as a function of centrality, when one goes from the very peripheral up to the most central Pb–Pb collisions.

In Fig. 17, the β exponents determined by a power law fit are displayed. In order to test the validity of the power law assumption, we have varied the centrality interval used

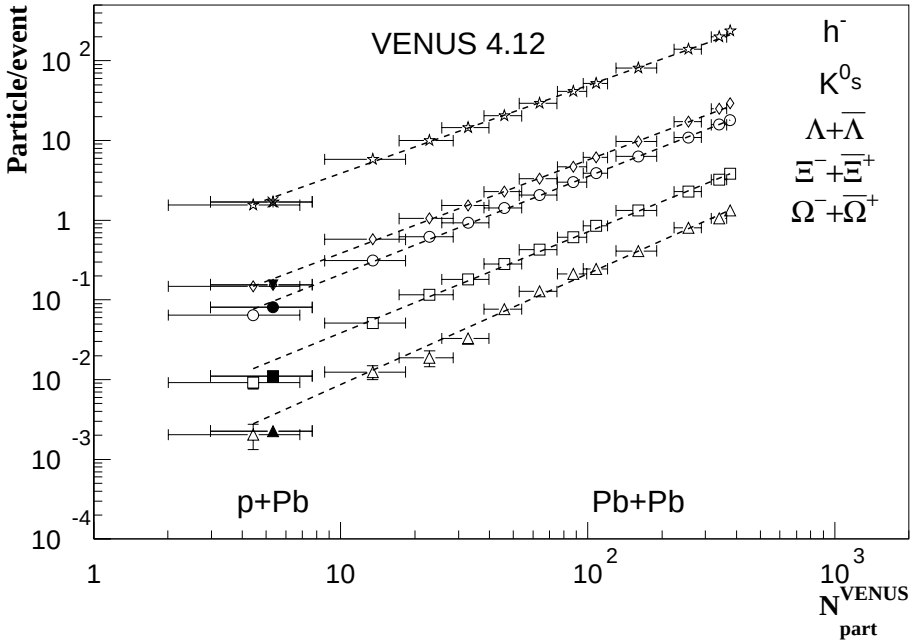

Fig. 15. The h^-, K^0_S, Λ, Ξ, and Ω yields as a function of the number of participants in VENUS-generated events

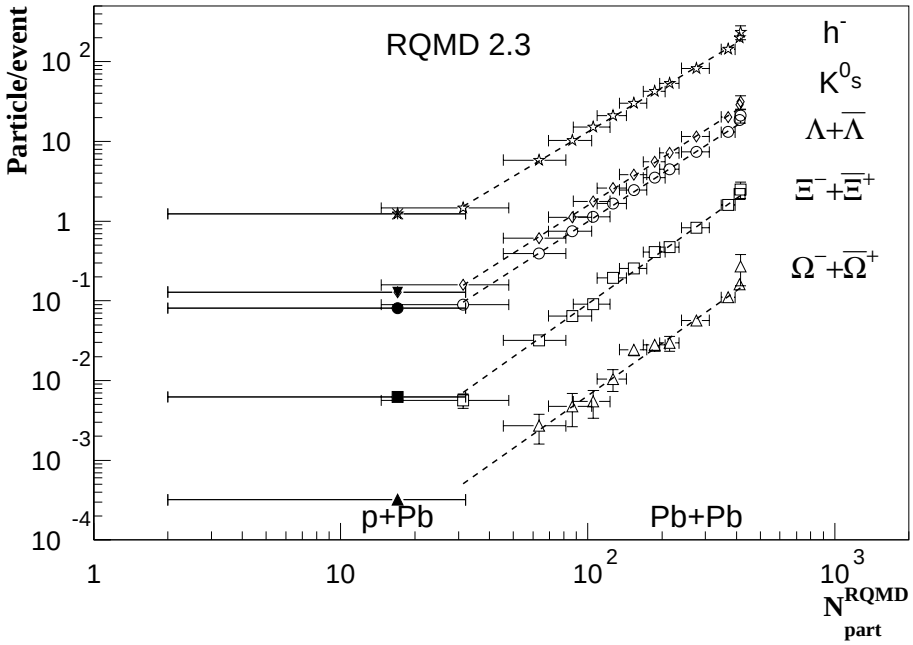

Fig. 16. The h^-, K^0_S, Λ, Ξ, and Ω yields as a function of the number of participants in RQMD generated events

in the fit. The black stars represent the result of a fit using all twelve Pb–Pb points of Figs. 15 and 16, while the open stars represent the result of a fit using the last four Pb–Pb points of the same figures. The β values shown in Fig. 12d and 12f (nonminimum bias) are also reported for comparison, as open squares and open circles, respectively.

The β values obtained from the 12-point fit remain substantially different from unity for both the models; this indicates that the increase of particle yields occurs faster than linearly with $N_{\rm part}$. Moreover, they exhibit a clear dependence on the particle mass; i.e., the Pb–Pb yields, as has already been noted, increase with centrality more rapidly as the strangeness content of the particle increases.

Comparing the β values obtained from the 12-point fit with those determined by a fit through the last four yield point, one can see that they do not change within the errors for RQMD. For VENUS, on the other hand, they do change and become compatible for all particles. This indicates that the VENUS increase of particle yields is not uniform throughout the centrality range of Pb–Pb collisions and tends to occur with the same slope for all the considered particles for very central events. Therefore the power law assumption is in this case inadequate.

Finally, the comparison of the β determined by a fit through the last four points with those shown in Fig. 12d and 12f shows how β depends on the centrality scale adopted. The β values are only slightly affected by a change

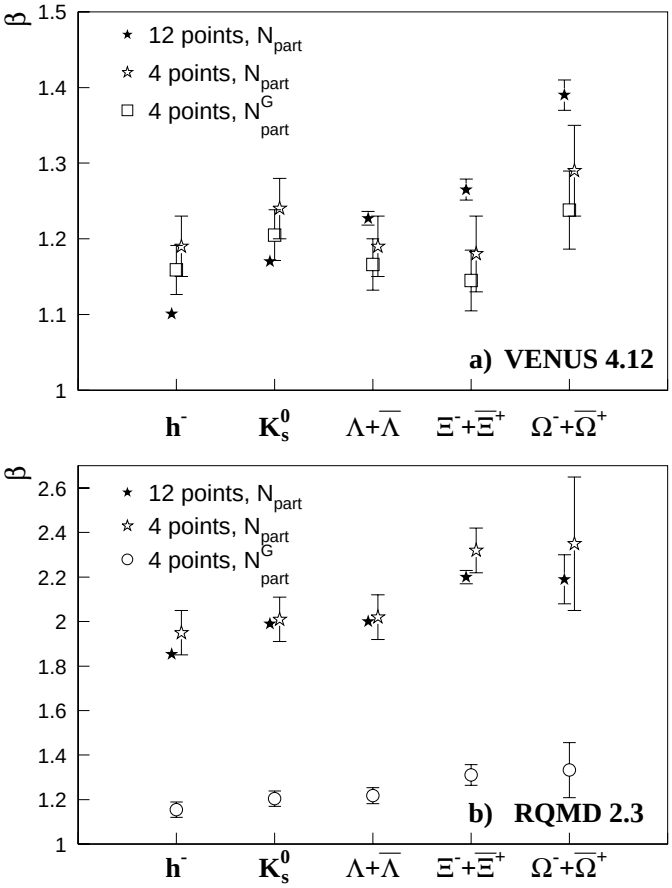

Fig. 17a,b. The β exponent determined by a power law fit under different conditions (see text for details) for VENUS yields **a** and RQMD yields **b**

from $N_{\rm part}^{\rm G}$ to $N_{\rm part}^{\rm VENUS}$, while they are shifted downwards when changing from $N_{\rm part}^{\rm G}$ to $N_{\rm part}^{\rm RQMD}$. It is interesting, however, to note that in both cases, the change of scale has little influence on the ratios of yields as a function of centrality.

In summary, both models exhibit a continuous increase of particle yields with $N_{\rm part}$, without any sudden change in slope, nor any saturation of strangeness production at high centrality.

6 Conclusions

A comparison of recent WA97 data on strangeness production at central rapidity in p–Pb and Pb–Pb collisions at 158 A GeV/c with two of the most used event generators, VENUS 4.12 and RQMD 2.3, has shown that:

- For p–Pb interactions, both models (Fig. 7) predict inverse slope parameters in fair agreement with WA97 data for h^-, $\overline{\Lambda}$, and $\overline{\Xi}^+$. They fail to reproduce K_S^0, Λ, and Ξ^- slopes.
  For Pb–Pb interactions (Fig. 9), VENUS and RQMD inverse slope parameters are globally in good agreement with WA97 data for all the considered particles.
- For p–Pb interactions (Figs. 6,8), VENUS fails to reproduce multistrange-particle yields. Ξ and Ω multiplicities are overestimated with respect to real data, the difference being larger as one goes from Ξ to Ω and from particles to antiparticles, up to one order of magnitude. RQMD yields are in agreement with the data. For Pb–Pb interactions, both models predict that enhancements increase with the strangeness content of the particle, a conclusion that is in qualitative agreement with the data. VENUS still overestimates the multistrange yields, while RQMD is able to reproduce all the measured yields, with the exception of the Ω, which are underestimated by a factor of 2.
- When compared in the same experimental conditions (Fig. 12), the models predict a steeper dependence on $N_{\rm part}^{\rm G}$ than the data, with β values clearly incompatible with one and larger than those measured by WA97.
- Finally, the models predict a continuous increase of negative and strange-particle production going from p–Pb up to very central Pb–Pb collisions. This trend appears to be in disagreement with WA97 results, which, at the present statistics, suggest a saturation of strangeness production at high centralities.

Acknowledgements. We are grateful to U. Heinz for fruitful discussions.

References

1. P. Koch, B. Müller, and J. Rafelski, Phys. Rep. **142**, 167 (1986)
2. J. Rafelski and B. Müller, Phys. Rev. Lett. **56**, 2334 (1986)
3. J. Rafelski, Phys. Lett. **B262**, 333 (1991)
4. S. Abatzis, et al. (WA85 Collaboration), Phys. Lett. **B376**, 251–254 (1996); A. Abatzis, et al. (WA94 Collaboration), Phys. Lett. **B400**, 239–244 (1997); L.S. Barnby, et al. (NA49 Collaboration), J. Phys. G **25**, 2469–2472 (1999)
5. E. Andersen, et al., Phys. Lett. **B433**, 209–216 (1998)
6. K. Werner, Phys. Rep. **232**, 87 (1993)
7. H. Sorge, Phys. Rev. **C52**, 3291 (1995)
8. Y. Pang, Nucl. Phys. **A638**, 219c–230c (1998)
9. T. Virgili, et al. (WA97 Collaboration), in *Proceedings of the International Conference on Strangeness in Quark Matter, Padova, Italy, July 20–24, 1998*, published in J. Phys. **G25**, 345–349 (1999)
10. F. Antinori, et al., Nucl. Phys. **A590** (1995) 139c.
11. R. Caliandro, et al. (WA97 Collaboration), in *Proceedings of the International Conference on Strangeness in Quark Matter, Padova, Italy, July 20–24, 1998*, published in J. Phys. **G25**, 171–180 (1999)
12. R. Lietava, et al. (WA97 Collaboration), in *Proceedings of the International Conference on Strangeness in Quark Matter, Padova, Italy, July 20–24, 1998*, published in J. Phys. **G25**, 181–188 (1999)
13. A. Capella, et al., Z. Phys. **C33**, 541 (1987)
14. B. Anderson, et al., Nucl. Phys. **B281**, 289 (1987)
15. M. Gonin, et al., Phys. Rev. **C51**, 310–317 (1995)
16. R. Brun, et al., GEANT3, CERN program library Q123
17. H. van Hecke, H. Sorge, and N. Xu, Phys. Rev. Lett. **81**, 5764 (1998)